iomac
International Operational Modal Analysis Conference

11th International Operational Modal Analysis Conference

20 - 23 May 2025 | Rennes, France

# Modal parameter extraction via the Loewner Framework: Current progress and future directions

*Gabriele Dessena* [*1] *and Marco Civera* [2]

[1] *Department of Aerospace Engineering, Universidad Carlos III de Madrid, Leganés, 28911, Madrid, Spain.*
GDessena@ing.uc3m.es
[2] *Department of Structural, Geotechnical and Building Engineering, Politecnico di Torino, 10129, Turin, Italy.*
Marco.Civera@polito.it
[*] *Corresponding Author*

**ABSTRACT**
Frequency-domain data continues to be widely employed in modal analysis, primarily due to its simplicity and intuitive interpretation. In particular, for simpler systems, an experienced practicioner can often directly discern system modes from frequency response functions. However, widely used methods such as rational fraction polynomial (RFP) and least-squares complex exponential (LSCE) can suffer from ill-conditioning, potentially obscuring critical structural dynamics. Meanwhile, time-domain techniques like subspace state-space system identification (N4SID) become expensive when analyzing large systems, raising concerns in aerospace applications demanding high accuracy and robustness. As a solution, the Loewner Framework (LF) has emerged as a robust, highly noise-robust alternative for extracting modal parameters. Initially, LF focused on single-input multi-output (SIMO) system identification, particularly in applications related to structural health monitoring. Originating from research on model order reduction in electronics and aerodynamics, the efficiency of the Loewner Framework (LF) has been effectively demonstrated across aeronautical, mechanical, and civil engineering applications. Furthermore, advanced formulations of LF now support the analysis of multiple-input, multiple-output (MIMO) and output-only datasets, showcasing its scalability. This work revisits the theoretical foundations of LF, critically assesses its advantages and limitations, and proposes avenues toward achieving comprehensive, efficient, and automated modal analysis.

*Keywords: Tangential Interpolation, Modal Analysis, Loewner Framework, Aerospace structures, Structural Health Monitoring*

## 1. INTRODUCTION

Modal analysis plays an important role in the design and validation of engineering systems across various fields. In particular, depending on the use case, the extraction of modal parameters can come from either Experimental Modal Analysis (EMA) or Operational Modal Analysis (OMA). While the aim remains the extraction of modal parameters – natural frequencies ($\omega_n$), damping ratios ($\zeta_n$), and mode shapes ($\phi_n$) – the key distinction is that in EMA, the input is known, whereas in OMA, it is either unknown or impossible to measure directly. For accommodating these scenarios a plethora of system identification methods, some more successful than others, have been proposed. The current state of the art method in the frequency domain are the likes of the Polyreference least-squares complex frequency-domain method (PolyMAX - although, only a commercial implementation is available) [1], the rational fraction polynomial (RFP) [2] and the least-squares complex exponential (LSCE - although it fits the impulse response function, IRF) [3], while in the time domain, the most popular techniques are the Numerical algorithm for (4) subspace state space System IDentification (N4SID - input-output) and Stochastic Subspace Identification with Canonical Variate Analysis (SSI - output-only) [4]. In recent years, several new techniques have been introduced to overcome the shortcomings, such as the fitting problem in the frequency domain and the noise robustness in the time domain, of existing methods. For example, In [5], a robust formulation of the covariance-driven variant of stochastic subspace identification (Cov-SSI) is introduced, exploiting a probabilistic approach to limit the risk of classifying outliers as actual physical modes. A Bayesian framework for OMA of systems with closely spaced modes is presented in [6], illustrating its effectiveness on a suspension footbridge. Furthermore, the Fast Relaxed Vector Fitting algorithm, originally a single-input multi-output (SIMO) method widely employed in electrical engineering, has been successfully adapted for modal identification [7] and vibration-based SHM [8], benefitting from its high computational efficiency. In this wave of new techniques, the Loewner Framework (LF) [9], also coming from electrical engineering, has established itself as a viable and robust alternative for modal parameter extraction [10]. Thus, this work covers the LF development as a modal analysis technique, its current progress, and the ongoing developments for its improvement.

## 2. THE LOEWNER FRAMEWORK

The LF is based on the Loewner matrix $\mathbb{L}$, first introduced by Karl Löwner in the 1930s. The matrix $\mathbb{L}$ can be seen as a generalized Hankel matrix for rational interpolation in the tangential direction.[1] Such that, its properties were then exploited by *Antoulas and co-authors* to develop a data-driven solution to the generalised realisation problem [9]; thus, proposing the LF. At the turn of the eighties, the $\mathbb{L}$ was first proposed as a tool for the solution of the minimal state-variable realisation problem from interpolation data in the frequency domain, although not yet considering tangential interpolation [12, 13]. This was not addressed until 2007, when in [9] the *Shifted Loewner matrix* ($\mathbb{L}_s$) was introduced to allow the realisation to be based on tangential interpolation and introducing the modern version of the LF considered in this work. Later, this allowed for the LF first real-world scenario application to the modelling of multiport-systems in Electrical Engineering [14, 15] and its seamless application of numerical model order reduction [16]. These were then followed by an application to aeroservoelastic systems in [17]. Through the years, also a time domain variant of the LF was also proposed [18], but it has yet to attract the same interest as its frequency domain counterpart. The most recent works on the formal development of the LF have focused on its application to nonlinear systems, such as Hammerstein cascaded dynamical systems [19], and to more efficient, matrix-less implementations [20]. In the remainder of this section, the mathematical background and structure of the conventional LF is presented.

Let us begin by defining the Loewner matrix $\mathbb{L}$: *Given a row array of pairs of complex numbers ($\mu_j$,$v_j$), $j = 1,...,q$, and a column array of pairs of complex numbers ($\lambda_i$,$w_j$), $i = 1,...,k$, with $\lambda_i$, $\mu_j$ distinct, the*

[1] This is also known as tangential interpolation [11].

*associated $\mathbb{L}$, or divided-differences matrix is:*

$$\mathbb{L} = \begin{bmatrix} \frac{\mathbf{v}_1 - \mathbf{w}_1}{\mu_1 - \lambda_1} & \dots & \frac{\mathbf{v}_1 - \mathbf{w}_k}{\mu_1 - \lambda_k} \\ \vdots & \ddots & \vdots \\ \frac{\mathbf{v}_q - \mathbf{w}_1}{\mu_q - \lambda_1} & \dots & \frac{\mathbf{v}_q - \mathbf{w}_k}{\mu_q - \lambda_k} \end{bmatrix} \in \mathbb{C}^{q \times k} \tag{1}$$

*If there is a known underlying function $\boldsymbol{\phi}$, then $\mathbf{w}_i = \boldsymbol{\phi}(\lambda_i)$ and $\mathbf{v}_j = \boldsymbol{\phi}(\mu_j)$.*

It is then possible to define interpolants based on determinants of submatrices of $\mathbb{L}$. According to [9, 21], rational interpolants can be derived from $\mathbb{L}$. The approach based on the Loewner pencil is considered in this work. The Loewner pencil consists of the $\mathbb{L}$ and $\mathbb{L}_s$ matrices, where $\mathbb{L}_s$ is the *Shifted Loewner matrix*, defined later.

To describe how the LF works, let us consider a linear time-invariant dynamical system $\boldsymbol{\Sigma}$ with $m$ inputs and $p$ outputs, and $k$ internal variables in descriptor-form representation, given by:

$$\boldsymbol{\Sigma}: \ \mathbf{E}\frac{d}{dt}\mathbf{x}(t) = \mathbf{A}\mathbf{x}(t) + \mathbf{B}\mathbf{u}(t); \quad \mathbf{y}(t) = \mathbf{C}\mathbf{x}(t) + \mathbf{D}\mathbf{u}(t) \tag{2}$$

where $\mathbf{x}(t) \in \mathbb{R}^k$ is the internal variable, $\mathbf{u}(t) \in \mathbb{R}^m$ is the function's input and $\mathbf{y}(t) \in \mathbb{R}^p$ is the output. The constant system matrices are:

$$\mathbf{E}, \mathbf{A} \in \mathbb{R}^{k \times k}, \ \mathbf{B} \in \mathbb{R}^{k \times m} \ \mathbf{C} \in \mathbb{R}^{p \times k} \ \mathbf{D} \in \mathbb{R}^{p \times m} \tag{3}$$

a Laplace transfer function, $\mathbf{H}(s)$, of $\boldsymbol{\Sigma}$ can be defined in the form of a $p \times m$ rational matrix function, when the matrix $\mathbf{A} - \lambda\mathbf{E}$ is non singular for a given finite value $\lambda$, such that $\lambda \in \mathbb{C}$:

$$\mathbf{H}(s) = \mathbf{C}(s\mathbf{E} - \mathbf{A})^{-1}\mathbf{B} + \mathbf{D} \tag{4}$$

Let us consider the more general case of tangential interpolation. The right interpolation data becomes:

$$(\lambda_i; \mathbf{r}_i, \mathbf{w}_i), \ i = 1, \dots, \rho \qquad \left.\begin{array}{c} \boldsymbol{\Lambda} = \text{diag}[\lambda_1, \dots, \lambda_k] \in \mathbb{C}^{\rho \times \rho} \\ \mathbf{R} = [\mathbf{r}_1 \ \dots \mathbf{r}_k] \in \mathbb{C}^{m \times \rho} \\ \mathbf{W} = [\mathbf{w}_1 \ \dots \ \mathbf{w}_k] \in \mathbb{C}^{\rho \times \rho} \end{array}\right\} \tag{5}$$

Likewise, the left interpolation data:

$$(\mu_j, \mathbf{l}_j, \mathbf{v}_j), \ j = 1, \dots, v \qquad \left.\begin{array}{c} \mathbf{M} = \text{diag}[\mu_1, \dots, \mu_q] \in \mathbb{C}^{v \times v} \\ \mathbf{L}^T = [\mathbf{l}_1 \ \dots \mathbf{l}_v] \in \mathbb{C}^{p \times v} \\ \mathbf{V}^T = [\mathbf{v}_1 \ \dots \ \mathbf{v}_q] \in \mathbb{C}^{m \times v} \end{array}\right\} \tag{6}$$

$\lambda_i$ and $\mu_j$ are the values at which $\mathbf{H}(s)$ is evaluated (the frequency bins in this application). The vectors $\mathbf{r}_i$ and $\mathbf{l}_j$ are, respectively, the right and left tangential general directions, randomly selected in practice [17], and $\mathbf{w}_i$ and $\mathbf{v}_j$ are the right and left tangential data. Linking $\mathbf{w}_i$ and $\mathbf{v}_j$ to the transfer function $\mathbf{H}$, associated with realisation $\boldsymbol{\Sigma}$ in Equation (2), solves the rational interpolation problem:

$$\mathbf{H}(\lambda_i)\mathbf{r}_i = \mathbf{w}_i, \ j = 1. \dots, \rho \quad \text{and} \quad \mathbf{l}_i\mathbf{H}(\mu_j) = \mathbf{v}_j, \ i = 1, \dots, v \tag{7}$$

such that the Loewner pencil satisfies Equation (7).

Now, let us consider a set of points $Z = \{z_1, \dots, z_N\}$ in the complex plane, a rational function $\mathbf{y}(s)$, such that $\mathbf{y}_i := \mathbf{y}(z_i), i = 1, \dots, N$, and let $Y = \{\mathbf{y}_1, \dots, \mathbf{y}_N\}$. Including the left and right data partitions, the following is obtained:

$$Z = \{\lambda_1, \ldots, \lambda_\rho\} \cup \{\mu_1, \ldots, \mu_v\} \quad \text{and} \quad Y = \{\mathbf{w}_1, \ldots, \mathbf{w}_\rho\} \cup \{\mathbf{v}_1, \ldots, \mathbf{v}_v\} \tag{8}$$

with $N = p + v$. Thus, the matrix $\mathbb{L}$ becomes:

$$\mathbb{L} = \begin{bmatrix} \frac{\mathbf{v}_1\mathbf{r}_1 - \mathbf{l}_1\mathbf{w}_1}{\mu_1 - \lambda_1} & \cdots & \frac{\mathbf{v}_1\mathbf{r}\rho - \mathbf{l}_1\mathbf{w}\rho}{\mu_1 - \lambda\rho} \\ \vdots & \ddots & \vdots \\ \frac{\mathbf{v}_v\mathbf{r}_1 - \mathbf{l}_v\mathbf{w}_1}{\mu_v - \lambda_1} & \cdots & \frac{\mathbf{v}_v\mathbf{r}\rho - \mathbf{l}_v\mathbf{w}\rho}{\mu_v - \lambda\rho} \end{bmatrix} \in \mathbb{C}^{v \times \rho} \tag{9}$$

Since $\mathbf{v}_v\mathbf{r}_p$ and $\mathbf{l}_v\mathbf{w}_p$ are scalars, the Sylvester equation is satisfied by $\mathbb{L}$ as follows:

$$\mathbb{L}\mathbf{\Lambda} - \mathbf{M}\mathbb{L} = \mathbf{L}\mathbf{W} - \mathbf{V}\mathbf{R} \tag{10}$$

Now, Let us define the *shifted Loewner matrix*, $\mathbb{L}_s$, as the $\mathbb{L}$ corresponding to $s\mathbf{H}(s)$:

$$\mathbb{L}_s = \begin{bmatrix} \frac{\mu_1\mathbf{v}_1\mathbf{r}_1 - \lambda_1\mathbf{l}_1\mathbf{w}_1}{\mu_1 - \lambda_1} & \cdots & \frac{\mu_1\mathbf{v}_1\mathbf{r}_\rho - \lambda_\rho\mathbf{l}_1\mathbf{w}_\rho}{\mu_1 - \lambda_\rho} \\ \vdots & \ddots & \vdots \\ \frac{\mu_v\mathbf{v}_v\mathbf{r}_1 - \lambda_1\mathbf{l}_v\mathbf{w}_1}{\mu_v - \lambda_1} & \cdots & \frac{\mathbf{v}_v\mathbf{r}_\rho - \mathbf{l}_v\mathbf{w}_\rho}{\mu_v - \lambda_\rho} \end{bmatrix} \in \mathbb{C}^{v \times \rho} \tag{11}$$

Likewise, the Sylvester equation is satisfied as follows:

$$\mathbb{L}_s\Lambda - \mathbf{M}\mathbb{L}_s = \mathbf{L}\mathbf{W}\mathbf{\Lambda} - \mathbf{M}\mathbf{V}\mathbf{R} \tag{12}$$

Let us focus on considering Equation (4) and matrix $\mathbf{D}$. As shown in [9], $\mathbf{D}$ is set to 0 per convention as its contributions are incorporated in the other matrices. So, Equation (4) becomes:

$$\mathbf{H}(s) = \mathbf{C}(s\mathbf{E} - \mathbf{A})^{-1}\mathbf{B} \tag{13}$$

A realisation with the smallest possible dimension exists only if the system is fully controllable and observable. Therefore, assuming the data is sampled from a system whose transfer function is characterised by Equation (13), the generalised tangential observability, $\mathcal{O}_v$, and generalised tangential controllability, $\mathcal{R}_\rho$, are defined as follows [15]:

$$\mathcal{O}_v = \begin{bmatrix} \mathbf{l}_1\mathbf{C}(\mu_1\mathbf{E} - \mathbf{A})^{-1} \\ \vdots \\ \mathbf{l}_v\mathbf{C}(\mu_q\mathbf{E} - \mathbf{A})^{-1} \end{bmatrix} \in \mathbb{R}^{v \times n} \tag{14}$$

$$\mathcal{R}_\rho = \begin{bmatrix} (\lambda_1\mathbf{E} - \mathbf{A})^{-1}\mathbf{B}\mathbf{r}_1 & \cdots & (\lambda_\rho\mathbf{E} - \mathbf{A})^{-1}\mathbf{B}\mathbf{r}_\rho \end{bmatrix} \in \mathbb{R}^{n \times \rho} \tag{15}$$

Now, let us incorporate Equations (14) and (15) into, respectively, Equations (9) and (11):

$$\mathbb{L}_{j,i} = \frac{\mathbf{v}_j\mathbf{r}_i - \mathbf{l}_j\mathbf{w}_i}{\mu_j - \lambda_i} = \frac{\mathbf{l}_j\mathbf{H}(\mu_i)\mathbf{r}_i - \mathbf{l}_j\mathbf{H}(\lambda_i)\mathbf{r}_i}{\mu_j - \lambda_i} = -\mathbf{l}_j\mathbf{C}(\mu_j\mathbf{E} - \mathbf{A})^{-1}\mathbf{E}(\lambda_i\mathbf{E} - \mathbf{A})^{-1}\mathbf{B}\mathbf{r}_i \tag{16}$$

$$(\mathbb{L}_s)_{j,i} = \frac{\mu_j \mathbf{v}_j - \lambda_i \mathbf{l}\mathbf{w}_i}{\mu_j - \lambda_i} = \frac{\mu_j \mathbf{l}_j \mathbf{H}(\mu_i)\mathbf{r}_i - \lambda_i \mathbf{l}_j \mathbf{H}(\lambda_i)\mathbf{r}_i}{\mu_j - \lambda_i} = \\ = -\mathbf{l}_j \mathbf{C}(\mu_j \mathbf{E} - \mathbf{A})^{-1}\mathbf{A}(\lambda_i \mathbf{E} - \mathbf{A})^{-1}\mathbf{B}\mathbf{r}_i \tag{17}$$

Firstly, let us consider the case with a minimal amount of data, where it is assumed that $p = v$. This assumption is based on the fact that no duplicate data is permitted in $\mathbf{R}$ and $\mathbf{L}$. Thus, rearranging Equations (14) and (15) into (16) and (17):

$$\mathbb{L} = -\mathcal{O}_v \mathbf{E} \mathcal{R}_\rho \qquad\qquad \mathbb{L}_s = -\mathcal{O}_v \mathbf{A} \mathcal{R}_\rho \tag{18}$$

Then, letting the Loewner pencil be a regular pencil, in the sense of $\mathrm{eig}((\mathbb{L}, \mathbb{L}_s)) \neq (\mu_i, \lambda_i)$:

$$\mathbf{E} = -\mathbb{L}, \qquad \mathbf{A} = -\mathbb{L}_s, \qquad \mathbf{B} = \mathbf{V}, \qquad \mathbf{C} = \mathbf{W} \tag{19}$$

Accordingly, the interpolating rational function is defined as follows:

$$\mathbf{H}(s) = \mathbf{W}(\mathbb{L}_s - s\mathbb{L})^{-1}\mathbf{V} \tag{20}$$

The derivation presented applies to the minimal data scenario, a case rarely encountered in real-world datasets. Nevertheless, the LF can be expanded to handle redundant data points effectively.

Firstly, let us assume:

$$\mathrm{rank}[\zeta\mathbb{L} - \mathbb{L}_s] = \mathrm{rank}[\mathbb{L}\ \mathbb{L}_s] == \mathrm{rank}\begin{bmatrix}\mathbb{L} \\ \mathbb{L}_s\end{bmatrix} = k,\ \forall \zeta \in \{\lambda_j\} \cup \{\mu_i\} \tag{21}$$

Secondly, the short Singular Value Decomposition (SVD) of $\zeta\mathbb{L} - \mathbb{L}_s$ is computed:

$$\mathrm{svd}(\zeta\mathbb{L} - \mathbb{L}_s) = \mathbf{Y}\mathbf{\Sigma}_l\mathbf{X} \tag{22}$$

where $\mathrm{rank}(\zeta\mathbb{L} - \mathbb{L}_s) = \mathrm{rank}(\mathbf{\Sigma}_l) = \mathrm{size}(\mathbf{\Sigma}_l) = k$, $\mathbf{Y} \in \mathbb{C}^{v \times k}$ and $\mathbf{X} \in \mathbb{C}^{k \times \rho}$. Thirdly, note that:

$$-\mathbf{A}\mathbf{X} + \mathbf{E}\mathbf{X}\mathbf{\Sigma}_l = \mathbf{Y}^*\mathbb{L}_s\mathbf{X}^*\mathbf{X} - \mathbf{Y}^*\mathbb{L}\mathbf{X}^*\mathbf{X}\mathbf{\Sigma}_l = \mathbf{Y}^*(\mathbb{L}_s - \mathbb{L}\mathbf{\Sigma}_l) = \mathbf{Y}^*\mathbf{V}\mathbf{R} = \mathbf{B}\mathbf{R} \tag{23}$$

and likewise, $-\mathbf{Y}\mathbf{A} + \mathbf{M}\mathbf{Y}\mathbf{E} = \mathbf{L}\mathbf{C}$ such that $\mathbf{X}$ and $\mathbf{Y}$ are, respectively, the generalised controllability and observability matrices for the system $\mathbf{\Sigma}$ with $\mathbf{D} = 0$. After verifying the right and left interpolation conditions, the Loewner realisation for redundant data is given by:

$$\mathbf{E} = -\mathbf{Y}^*\mathbb{L}\mathbf{X}, \qquad \mathbf{A} = -\mathbf{Y}^*\mathbb{L}_s\mathbf{X}, \qquad \mathbf{B} = \mathbf{Y}^*\mathbf{V}, \qquad \mathbf{C} = \mathbf{W}\mathbf{X} \tag{24}$$

The formulation of Equation (24) — that is, the Loewner realisation for redundant data — is considered in this work. For a more detailed discussion of each step, the interested reader is referred to [9, 21].

## 3. CURRENT PROGRESS

After outlining the structure and background of the Loewner Framework (LF), it is important to clarify the authors' specific contribution to its application in modal analysis, which was to allow the extraction of a system modal parameters. This was obtained by eigenanalysis of the system matrices $\mathbf{A}$ and $\mathbf{C}$ from Equation (24). This breakthrough allowed us to pioneeringly apply the LF for the extraction of modal parameters [10, 22] from the well-known 3 degrees of freedom (DoFs) experimental benchmark of the three-storey structure (Figure 1) from the Los Alamos National Laboratory [23]. The benchmark contained a detailed dataset of 17 cases (each including 50 repetitions of the same test) of a random

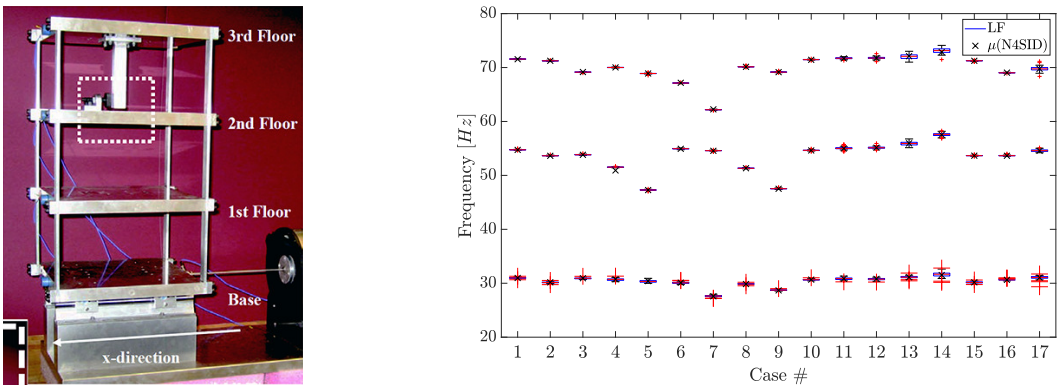


*(a)* *(b)*

**Figure 1:** Modal identification of the three-storey structure: Figure 1a (Adapted from [23]) shows the experimental structure and Figure 1b the identified $\omega_n$ from the 17 cases, across the 50 test repetitions (Retrieved from [10]).

vibration test of a shear structure. The cases mimic either damage, simulated as the addition of mass and/or stiffness reduction in the interstorey columns, or nonlinear scenarios.

Here, the LF-identified modal parameters were coherent with those presented in the benchmark original work [23], other subsequent works [8], and those identified with N4SID as a benchmark. This confirmed that the LF was sufficiently accurate to succesfulyy perform vibration-based SHM applications. Furthermore, the LF was shown to work much better than LSCE for the identification of close-in-frequency modes on a 9 DoFs numerical system.

After validating the method application to modal analysis, its performance, in terms of computational time was assessed in [24]. Here the time-to-identification of the newly proposed LF was compared to that of N4SID and LSCE and it was found that the LF is the best compromise in terms of cost-to-performance, as it was as precise as N4SID, while being quicker, and slightly slower (tenths of seconds) than LSCE, which could not identify close-in-frequency modes. This analysis used a hybrid, experimental and numerical, test case of an 8 DoFs mass-spring-damper system [25].

In [26], the LF robustness to noise is compared against that of the, also recently introduced, Fast Relaxed Vector Fitting (FRVF). This comparison is first carried out on a numerical system with added white Gaussian noise at different levels. Then, on a newly introduced SHM dataset of a flexible wing[2] known as XB-2, which details can be found in [27–29]. The LF was found to be more robust to noise than FRVF, but slightly less precise when compared with N4SID results. The modal parameters obtained from this work are then used in [30] to make a flutter speed prediction of XB-2.

One of the main limitations of the LF for modal parameter extraction was its single-input multi-output-only (SIMO-only) capability. To overcome this, a computationally improved version of the LF (iLF) was proposed [31], which not only accounts for multi-input multi-output (MIMO) systems, but reduces computational times by $10^{-1}$ without any penalty in accuracy and precision. This was validated on the recently introduced BAE Systems Hawk T1A aircraft benchmark [32] (Figure 2a) by identifying the modal parameters of its healthy state (also many damaged states, and input types, are available) and testing its robustness to noise on a numerical system. The $\phi_1$ identified from the experimental data are shown in Figure 2b. The large size of the experimental specimen (5 input and 85 output channels) seriously challenged LSCE and N4SID. The former not being to give any significant results, and the latter identifying up to two modes with a computational time of almost a day, against the few seconds of the iLF. The large dataset size was also found to be an issue also for SSI in [33], where vibration-based SHM is carried out using the modified total modal assurance criterion (MTMAC) as a standalone metric. SSI failed to identify the modes of interest.

[2]found at `https://doi.org/10.5281/zenodo.11635814`


*(a)* *(b)*

**Figure 2:** Modal identification of the BAE Systems T1A: Figure 2a (Retrieved from [32]) shows the BAE Systems T1A as instrumented for the MIMO tests and Figure 2b the $\phi_1$ identified from the MIMO data with 5 input and 85 output channels (Retrieved from [31]).

After MIMO capability, the only limitation was that now the LF could only be employed for EMA and not for OMA. Thus, in [34], the standard (SIMO-only) LF was paired with the Natural Excitation Technique (NExT) [35] to overcome this limitation. NExT works by mimicking a system IRF by computing the cross-correlation between all output channels time series and a given reference within those. These can then be brought into the frequency domain by means of a fast Fourier transform and obtain an equivalent FRF from an unknown input. Following this logic, NExT was paired to the LF to form NExT-LF, which was applied to a numerical system, for validating its noise robustness, and the real-life real-size case of the Sheraton Universal Hotel (North Hollywood, CA, in the USA – Figure 3a), a 54 m tall reinforced concrete building. This was the first time that modal parameters were identified from this structure. The $\phi_1$ identified by LF is shown in Figure 3b.

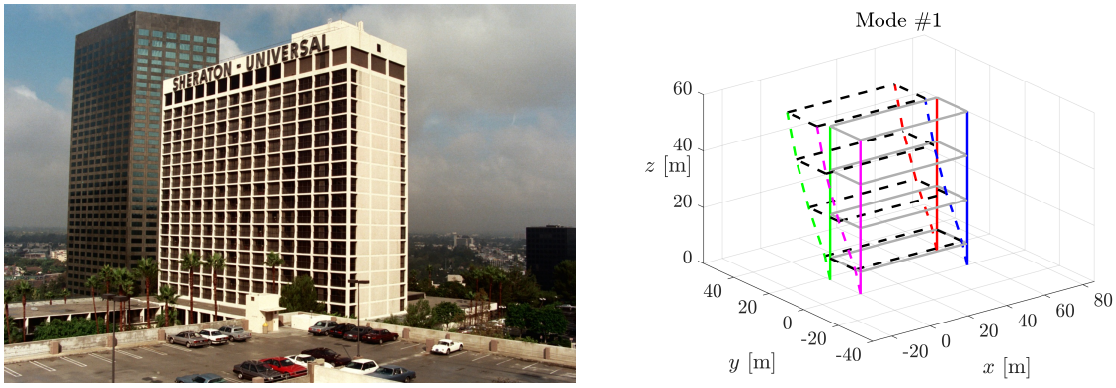


*(a)* *(b)*

**Figure 3:** Operational modal analysis of the Sheraton Universal Hotel: Figure 3a (Adapted from Flickr, Inc) shows the Sheraton Universal Hotel and Figure 3b the $\phi_1$ identified from the output-only data (Retrieved from [34]).

## 4. FUTURE DIRECTIONS

At the current state, modal parameters can be obtained via the LF from both known and unknown input scenarios. However, the development of this method is still underway as crucial improvements can be made to expand its use case scenarios. There are two main development directions for the future. The first is method improvement, both in computational and theoretical terms, and the second is automation. Concerning the first, the main ongoing developments concern the implementation of a matrix-less version of LF, as done in [20] for general system identification, and the implementation of a multi-reference

NExT-LF. The former would speed up the computational time and even allow for the identification of larger datasets, while the latter aims at making the output-only identification via the LF more robust by avoiding any potential bias induced by a single reference channel. On the automation side, although this is very much an idea in its infancy, the aim is to rely on the graphical representation brought by the stabilisation diagrams and use matrix-less partial orthogonal decomposition [36] to identify the dominant modes across various algorithm settings. The final idea is that these advances will allow us to move from a post-test towards a real- or quasi-real-time use of the LF to be used on operational aerospace systems, such as varying stiffness wings and reusable flexible launchers.

## 5. CONCLUSIONS

This work covers the story of the LF application to modal analysis, showing its maturity in the field that allows its application for both OMA and EMA, even for multi-input, scenarios. In particular, it demonstrates enhanced performance over existing state-of-the-art techniques, both in terms of computational efficiency and identification accuracy. Up to now, the LF has been successfully applied to simple benchmark systems, such as the three-storey structure and the 8 degrees-of-freedom mass-spring-damper from the Los Alamos National Laboratory, and complex real-life real-size structures, such as a full aircraft (BAE Systems Hawk T1A) and a 54 m tall reinforced concrete hotel. In addition, the identification results from LF have informed vibration-based structural health monitoring on many of these systems. Although the LF is a mature technique, current areas of development aim at improving even more its computational efficiency and its output-only capability, for allowing real- or quasi-real-time in-flight modal tracking of aeronautical and aerospace systems, such as aircraft and launch vehicles.

## ACKNOWLEDGEMENTS

The first author has been supported by the Madrid Government (*Comunidad de Madrid* – Spain) under the Multiannual Agreement with the Universidad Carlos III de Madrid (IA_aCTRl-CM-UC3M) and by UC3M Fundings for Research Activities (*Ayudas para la Actividad Investigadora de los Jóvenes Doctores, del Programa Propio de Investigación de la UC3M*). The second author is supported by the Centro Nazionale per la Mobilità Sostenibile (MOST – Sustainable Mobility Center), Spoke 7 (Cooperative Connected and Automated Mobility and Smart Infrastructures), Work Package 4 (Resilience of Networks, Structural Health Monitoring and Asset Management).

## REFERENCES

[1] Bart Peeters, Herman Van der Auweraer, Patrick Guillaume, and Jan Leuridan. The PolyMAX Frequency-Domain Method: A New Standard for Modal Parameter Estimation? *Shock and Vibration*, 11(3-4):395–409, jan 2004. ISSN 1070-9622. doi: 10.1155/2004/523692. URL https://onlinelibrary.wiley.com/doi/10.1155/2004/523692.

[2] Mark H. Richardson and David L. Formenti. Global curve fitting of frequency response measurements using the rational fraction polynomial method. *Proceedings of the International Modal Analysis Conference & Exhibit*, 1:390–397, 1985.

[3] Frank R. Spitznogle and Azizul H Quazi. Representation and Analysis of Time-Limited Signals Using a Complex Exponential Algorithm. *The Journal of the Acoustical Society of America*, 47 (5A):1150–1155, may 1970. ISSN 0001-4966. doi: 10.1121/1.1912020. URL https://pubs.aip.org/jasa/article/47/5A/1150/716351/Representation-and-Analysis-of-Time-Limited.

[4] Peter Van Overschee and Bart De Moor. *Subspace Identification for Linear Systems*. Number

November 2014. Springer US, Boston, MA, 1996. ISBN 978-1-4613-8061-0. doi: 10.1007/978-1-4613-0465-4. URL http://link.springer.com/10.1007/978-1-4613-0465-4.

[5] Brandon J. O'Connell and Timothy J. Rogers. A robust probabilistic approach to stochastic subspace identification. *Journal of Sound and Vibration*, 581(March):118381, jul 2024. ISSN 0022460X. doi: 10.1016/j.jsv.2024.118381. URL https://linkinghub.elsevier.com/retrieve/pii/S0022460X24001445.

[6] Zuo Zhu, Siu-Kui Au, Binbin Li, and Yan-Long Xie. Bayesian operational modal analysis with multiple setups and multiple (possibly close) modes. *Mechanical Systems and Signal Processing*, 150:107261, mar 2021. ISSN 08883270. doi: 10.1016/j.ymssp.2020.107261. URL https://linkinghub.elsevier.com/retrieve/pii/S0888327020306476.

[7] Marco Civera, Giulia Calamai, and Luca Zanotti Fragonara. Experimental modal analysis of structural systems by using the fast relaxed vector fitting method. *Structural Control and Health Monitoring*, 28(4):1–23, apr 2021. ISSN 1545-2255. doi: 10.1002/stc.2695. URL https://onlinelibrary.wiley.com/doi/10.1002/stc.2695.

[8] Marco Civera, Giulia Calamai, and Luca Zanotti Fragonara. System identification via fast relaxed vector fitting for the structural health monitoring of masonry bridges. *Structures*, 30(January): 277–293, apr 2021. ISSN 23520124. doi: 10.1016/j.istruc.2020.12.073.

[9] A.J. Mayo and A.C. Antoulas. A framework for the solution of the generalized realization problem. *Linear Algebra and its Applications*, 425(2-3):634–662, sep 2007. ISSN 00243795. doi: 10.1016/j.laa.2007.03.008. URL https://linkinghub.elsevier.com/retrieve/pii/S0024379507001280.

[10] Gabriele Dessena, Marco Civera, Luca Zanotti Fragonara, Dmitry I. Ignatyev, and James F. Whidborne. A Loewner-Based System Identification and Structural Health Monitoring Approach for Mechanical Systems. *Structural Control and Health Monitoring*, 2023:1–22, apr 2023. ISSN 1545-2263. doi: 10.1155/2023/1891062. URL https://www.hindawi.com/journals/schm/2023/1891062/.

[11] B. Kramer and S. Gugercin. Tangential interpolation-based eigensystem realization algorithm for MIMO systems. *Mathematical and Computer Modelling of Dynamical Systems*, 22(4):282–306, jul 2016. ISSN 1387-3954. doi: 10.1080/13873954.2016.1198389. URL https://www.tandfonline.com/doi/full/10.1080/13873954.2016.1198389.

[12] A.C. Antoulas and B.D.O. Anderson. On the problem of stable rational interpolation. *Linear Algebra and its Applications*, 122-124(C):301–329, sep 1989. ISSN 00243795. doi: 10.1016/0024-3795(89)90657-5. URL https://linkinghub.elsevier.com/retrieve/pii/0024379589906575.

[13] B.D.O. Anderson and A.C. Antoulas. Rational interpolation and state-variable realizations. *Linear Algebra and its Applications*, 137-138(C):479–509, aug 1990. ISSN 00243795. doi: 10.1016/0024-3795(90)90140-8. URL https://linkinghub.elsevier.com/retrieve/pii/0024379590901408.

[14] Sanda Lefteriu and Athanasios C. Antoulas. Modeling multi-port systems from frequency response data via tangential interpolation. In *2009 IEEE Workshop on Signal Propagation on Interconnects*, pages 1–4, may 2009. ISBN 978-1-4244-4490-8. doi: 10.1109/SPI.2009.5089847. URL http://ieeexplore.ieee.org/document/5089847/.

[15] Sanda Lefteriu and Athanasios C. Antoulas. A new approach to modeling multiport systems from frequency-domain data. *IEEE Transactions on Computer-Aided Design of Integrated Circuits and*

*Systems*, 29(1):14–27, jan 2010. ISSN 02780070. doi: 10.1109/TCAD.2009.2034500. URL http://ieeexplore.ieee.org/document/5356286/.

[16] Antonio C. Ionita and Athanasios C. Antoulas. Case Study: Parametrized Reduction Using Reduced-Basis and the Loewner Framework. In Alfio Quarteroni and Gianluigi Rozza, editors, *Reduced Order Methods for Modeling and Computational Reduction*, chapter 2, pages 51–66. Springer International Publishing, Cham, 2014. doi: 10.1007/978-3-319-02090-7_2. URL http://link.springer.com/10.1007/978-3-319-02090-7{_}2.

[17] David Quero, Pierre Vuillemin, and Charles Poussot-Vassal. A generalized state-space aeroservoelastic model based on tangential interpolation. *Aerospace*, 6(1):9, jan 2019. ISSN 2226-4310. doi: 10.3390/aerospace6010009. URL http://www.mdpi.com/2226-4310/6/1/9.

[18] Joel D. Simard and Alessandro Astolfi. Loewner functions for linear time-varying systems with applications to model reduction. *IFAC-PapersOnLine*, 53(2):5623–5628, 2020. ISSN 24058963. doi: 10.1016/j.ifacol.2020.12.1578. URL https://doi.org/10.1016/j.ifacol.2020.12.1578.

[19] Dimitrios S. Karachalios, Ion Victor Gosea, and Athanasios C. Antoulas. The Loewner framework for nonlinear identification and reduction of Hammerstein cascaded dynamical systems. *PAMM*, 20(1):2020–2022, jan 2021. ISSN 1617-7061. doi: 10.1002/pamm.202000337. URL https://onlinelibrary.wiley.com/doi/10.1002/pamm.202000337.

[20] Davide Palitta and Sanda Lefteriu. An Efficient, Memory-Saving Approach for the Loewner Framework. *Journal of Scientific Computing*, 91(2):31, may 2022. ISSN 0885-7474. doi: 10.1007/s10915-022-01800-3. URL https://link.springer.com/10.1007/s10915-022-01800-3.

[21] Athanasios C. Antoulas, Sanda Lefteriu, and A. Cosmin Ionita. A Tutorial Introduction to the Loewner Framework for Model Reduction. In *Model Reduction and Approximation*, number May 2011, chapter 8, pages 335–376. Society for Industrial and Applied Mathematics, Philadelphia, PA, jul 2017. ISBN 1545-2263. doi: 10.1137/1.9781611974829.ch8. URL http://epubs.siam.org/doi/10.1137/1.9781611974829.ch8.

[22] Gabriele Dessena. *Identification of flexible structures dynamics*. PhD thesis, Centre for Autonomous and Cyber-Physical Systems, Cranfield University, 2023. URL https://dspace.lib.cranfield.ac.uk/handle/1826/20261.

[23] Eloi Figueiredo, Gyuhae Park, Joaquim Figueiras, Charles Farrar, and Keith Worden. Structural health monitoring algorithm comparisons using standard data sets. Technical report, Los Alamos National Laboratory (LANL), Los Alamos, NM (United States), mar 2009. URL https://www.osti.gov/servlets/purl/961604/.

[24] Gabriele Dessena, Marco Civera, Dmitry I. Ignatyev, James F. Whidborne, Luca Zanotti Fragonara, and Bernardino Chiaia. The Accuracy and Computational Efficiency of the Loewner Framework for the System Identification of Mechanical Systems. *Aerospace*, 10(6):571, jun 2023. ISSN 2226-4310. doi: 10.3390/aerospace10060571. URL https://www.mdpi.com/2226-4310/10/6/571.

[25] Francois M. Hemez and Scott W. Doebling. Review and assessment of model updating for non-linear, transient dynamics. *Mechanical Systems and Signal Processing*, 15(1):45–74, jan 2001. ISSN 08883270. doi: 10.1006/mssp.2000.1351. URL https://linkinghub.elsevier.com/retrieve/pii/S0888327000913517.

[26] Gabriele Dessena, Marco Civera, Alessandro Pontillo, Dmitry I. Ignatyev, James F. Whidborne, and Luca Zanotti Fragonara. Noise-robust modal parameter identification and damage assessment for aero-structures. *Aircraft Engineering and Aerospace Technology*, 96(11):27–36, 2024. ISSN 1748-8842. doi: 10.1108/AEAT-06-2024-0178. URL https://www.emerald.com/insight/content/doi/10.1108/AEAT-06-2024-0178/full/html.

[27] Alessandro Pontillo. *High Aspect Ratio Wings on Commercial Aircraft: a Numerical and Experimental approach*. Phd thesis, Centre for Aeronautics, Cranfield University, 2020. URL https://dspace.lib.cranfield.ac.uk/handle/1826/20266.

[28] Gabriele Dessena, Dmitry I. Ignatyev, James F. Whidborne, Alessandro Pontillo, and Luca Zanotti Fragonara. Ground vibration testing of a flexible wing: A benchmark and case study. *Aerospace*, 9 (8):438, 2022. ISSN 2226-4310. doi: 10.3390/aerospace9080438. URL https://www.mdpi.com/2226-4310/9/8/438.

[29] Gabriele Dessena, Alessandro Pontillo, Dmitry I. Ignatyev, James F. Whidborne, and Luca Zanotti Fragonara. Identification of Nonlinearity Sources in a Flexible Wing. *Journal of Aerospace Engineering*, 2025. doi: 10.1061/JAEEEZ/ASENG-5508. URL https://doi.org/10.1061/JAEEEZ/ASENG-5508.

[30] Gabriele Dessena, Alessandro Pontillo, Marco Civera, Dmitry I. Ignatyev, James F. Whidborne, and Luca Zanotti Fragonara. Structural Damping Identification Sensitivity in Flutter Speed Estimation. *Vibration*, 2025. URL http://arxiv.org/abs/2503.04433.

[31] Gabriele Dessena and Marco Civera. Improved tangential interpolation-based multi-input multi-output modal analysis of a full aircraft. *European Journal of Mechanics - A/Solids*, 110(March-April):105495, mar 2025. ISSN 09977538. doi: 10.1016/j.euromechsol.2024.105495. URL https://linkinghub.elsevier.com/retrieve/pii/S0997753824002754.

[32] James Wilson, Max D. Champneys, Matt Tipuric, Robin Mills, David J. Wagg, and Timothy J. Rogers. Multiple-input, multiple-output modal testing of a Hawk T1A aircraft: a new full-scale dataset for structural health monitoring. *Structural Health Monitoring*, pages 1–23, dec 2024. ISSN 1475-9217. doi: 10.1177/14759217241297098. URL https://journals.sagepub.com/doi/10.1177/14759217241297098.

[33] Gabriele Dessena, Marco Civera, Andrés Marcos, and Bernardino Chiaia. Multi-input Multi-output Loewner Framework for Vibration-based Damage Detection on a Trainer Jet. *arXiv*, pages 1–29, oct 2024. doi: 10.48550/arXiv.2410.20160. URL http://arxiv.org/abs/2410.20160.

[34] Gabriele Dessena, Marco Civera, Ali Yousefi, and Cecilia Surace. NExT-LF: A Novel Operational Modal Analysis Method via Tangential Interpolation. *International Journal of Mechanical System Dynamics*, 2025. doi: 10.1002/msd2.70016. URL https://doi.org/10.1002/msd2.70016.

[35] George H James III, Thomas G Carne, and James P. Lauffer. The Natural Excitation Technique (NExT) for Modal Parameter Extraction From Operating Wind Turbines. Technical report, Sandia National Laboratories, Albuquerque, NM, 1993. URL http://energy.sandia.gov/download/23492/.

[36] Iacopo Tirelli, Miguel Alfonso Mendez, Andrea Ianiro, and Stefano Discetti. A meshless method to compute the proper orthogonal decomposition and its variants from scattered data. *Proceedings of the Royal Society A: Mathematical, Physical and Engineering Sciences*, 481:20240526, 2025. doi: 10.1098/rspa.2024.0526. URL https://doi.org/10.1098/rspa.2024.0526.